
Linear Connectivity Reveals Generalization Strategies

Jeevesh Juneja

Delhi Technological University
jeeveshjuneja@gmail.com

Rachit Bansal

Delhi Technological University
racbansa@gmail.com

Kyunghyun Cho

New York University
kyunghyun.cho@nyu.edu

João Sedoc

New York University
jsedoc@stern.nyu.edu

Naomi Saphra

New York University
nsaphra@nyu.edu

Abstract

It is widely accepted in the model connectivity literature that when two neural networks are trained similarly on the same data, they are connected by a path through parameter space over which test set accuracy is maintained. Under some circumstances, including transfer learning from pretrained models, these paths are presumed to be linear. In contrast to existing results, we find that among text classifiers (trained on MNLI, QQP, and CoLA), some pairs of finetuned models have large barriers of increasing loss on the linear paths between them. On each task, we find distinct clusters of models which are linearly connected on the test loss surface, but are disconnected from models outside the cluster—models that occupy separate basins on the surface. By measuring performance on specially-crafted diagnostic datasets, we find that these clusters correspond to different generalization strategies: one cluster behaves like a bag of words model under domain shift, while another cluster uses syntactic heuristics. Our work demonstrates how the geometry of the loss surface can guide models towards different heuristic functions.

1 Introduction

Modern training methods are capable of discovering high-performance parameters for neural networks on a variety of tasks. Although models trained with similar procedures tend to exhibit similar in-domain (ID) performance on these tasks, they exhibit diverse decision boundaries [1]. In particular, models with similar performance can make significantly different judgments when presented with examples that fall far from the training data manifold [43]. In computer vision, these discussions of generalization often focus on visualizations of decision boundaries learnt by the different models.

In NLP, generalization behavior is instead usually characterized structurally through the use of diagnostic sets. Previous studies of model behavior on out-of-distribution (OOD) linguistic structures show that finetuned models can exhibit variation in compositional generalization and performance on diagnostic sets [31, 56]. For example, in natural language inference tasks, some models seem to deploy strategies during OOD generalization that incorporate no position information at all [32]. To the best of our knowledge, these different generalization behaviors have never been linked to the geometry of the loss surface. In order to explore how barriers in the loss surface expose a model’s generalization strategy, we consider the case of text classification. We focus in particular on Natural Language Inference [NLI; 50, 3], as well as paraphrase and grammatical acceptability tasks.

We find that NLI models tend to rely on one of two strategies, both of which exhibit similar loss on the test set. We characterize these strategies as, roughly, **syntax-aware** and **syntax-unaware**.

They fall into two respective basins; the syntax-aware basin contains functions that tend to rely on heuristics around the behavior of constituents, while functions in the syntax-unaware basin rely on lexical bag-of-words heuristics. We find that in NLI, paraphrase, and grammaticality judgment tasks, models that perform similarly on the same diagnostic sets are linearly connected without barriers on the ID loss surface, but they tend to be disconnected from models with different generalization behavior. Our main contributions are:

- We formally define the notion of an ϵ -convex basin to describe sets of weights that can linearly connect to the same low-loss points without crossing large loss surface barriers (Section 3.1).
- We develop a metric based on linear mode connectivity, the **convexity gap** (Section 4), and an accompanying method for clustering models into basins (Section 4.1). In contrast with existing work in computer vision [35], we find that transfer learning can lead to different basins over different finetuning runs (Section 3).
- We align the basins to specific generalization behaviors. In NLI (Section 2.1), they correspond to a preference for either syntactic or lexical overlap heuristics (Section 4). On a paraphrase task (Section 2.2), the basins likewise split on behavior under word order permutation (Section 4.1.1). On a linguistic acceptability task, they reveal the ability to classify linguistic phenomena unseen during finetuning (Appendix A).
- We confirm that these basins trap a portion of finetuning runs, which become increasingly disconnected from the other models as they train (Section 4.2). Based on this behavior, it may be possible to predict final heuristics from early connectivity.

2 Identifying generalization strategies

Finetuning on standard GLUE [45] datasets often leads to models that perform similarly on in-domain (ID) test sets [40]. To evaluate the functional differences between these models, we need to evaluate their generalization to diagnostic datasets. In this paper, we study the variation of performance on these existing diagnostic datasets. We will call models with poor performance on the generalization set **heuristic models** while those with high performance will be **generalizing models**. We study three tasks with diagnostic sets: NLI, paraphrase, and linguistic acceptability (the latter in Appendix A).

2.1 Natural Language Inference

NLI is a common testbed for NLP models. This binary classification task poses a challenge in modeling both syntax and semantics. The input to an NLI model is a pair of sentences such as:

- *Premise*: The dog scared the cat.
- *Hypothesis*: The cat was scared by the dog.

Here, the label is positive or **entailment**, because the hypothesis can be inferred from the premise. If the hypothesis were, “The dog was scared by the cat”, the label would be negative or **non-entailment**. We use the MNLI [50] corpus, and inspect loss surfaces on the “matched” validation set.¹

NLI models often “cheat” by relying on heuristics, such as overlap between either individual lexical items or syntactic constituents shared by the premise and hypothesis. If a model relies on lexical overlap, both the entailed and non-entailed examples above might be given positive labels, because all three sentences contain “scared”, “dog”, and “cat”. McCoy et al. [32] responded to these shortcuts by creating HANS, a diagnostic set of sentence pairs that violate such heuristics:

- **Lexical overlap (HANS-LO)**: Entails any hypothesis containing the same words as the premise.
- **Subsequence**: Entails any hypothesis containing contiguous sequences of words from the premise.
- **Constituent**: Entails any hypothesis containing syntactic subtrees from the premise.

Unless otherwise specified, we use the non-entailing HANS subsets for measuring reliance on heuristics, so higher accuracy on HANS-LO indicates less reliance on lexical overlap.

¹An unmatched validation set is also available, which includes different sources and topics from the training set. The test set labels are not public for MNLI or QQP, so we use the validation set only.

2.2 Paraphrase

Quora Question Pairs [QQP; 47] is a common paraphrase corpus. The dataset contains 400k pairs of questions that have been annotated with a binary value indicating whether they are duplicates. We use the PAWS-QQP [54] dataset as the diagnostic set for identifying different generalization behaviors learnt by the models. PAWS-QQP contains QQP sentences that have been permuted in order to construct pairs that can mean different things, even though they have the same words. In other words, they are pairs that may violate a lexical overlap heuristic.

2.3 Experimental details

All models are initialized from bert-base-uncased,² with a linear classification head. Each model has a random seed determining both the initialisation of the linear layer and the data order. QQP models are trained with Google’s recommended default hyperparameters (details in Appendix F). MNLI models are those provided by McCoy et al. [31]. Both have been trained using Google’s original trainer.³

2.3.1 Computational resources

Finetuning 100 QQP models cost around 500 GPU-hours and 48 CoLA models cost around 10 GPU-hours. Each 100×100 interpolation and evaluation consumed 114 GPU hours; these were performed for both QQP (at three stages during finetuning, for Fig. 7) and MNLI. The 48×48 interpolation for CoLA cost about 28 GPU-hours. The experiments add up to a total cost of approximately 994 GPU-hours on a mix of NVIDIA RTX8000 and V100 nodes.

3 Linear Mode Connectivity

Models discovered by SGD are generally connected by paths over which the loss is maintained [6]. If we limit such paths to be linear, however, connectivity is no longer guaranteed. We may still find, however, that two parameter settings θ_A and θ_B , which achieve equal loss, can be connected by linear interpolation without any increase in loss [12]. In other words, loss $\mathcal{L}(\theta_\alpha; X_{\text{train}}, Y_{\text{train}}) \leq \mathcal{L}(\theta_A; X_{\text{train}}, Y_{\text{train}})$ and $\mathcal{L}(\theta_\alpha; X_{\text{train}}, Y_{\text{train}}) \leq \mathcal{L}(\theta_B; X_{\text{train}}, Y_{\text{train}})$ in each parameter setting θ_α defined by any scalar $0 \leq \alpha \leq 1$:

$$\theta_\alpha = \alpha\theta_A + (1 - \alpha)\theta_B \tag{1}$$

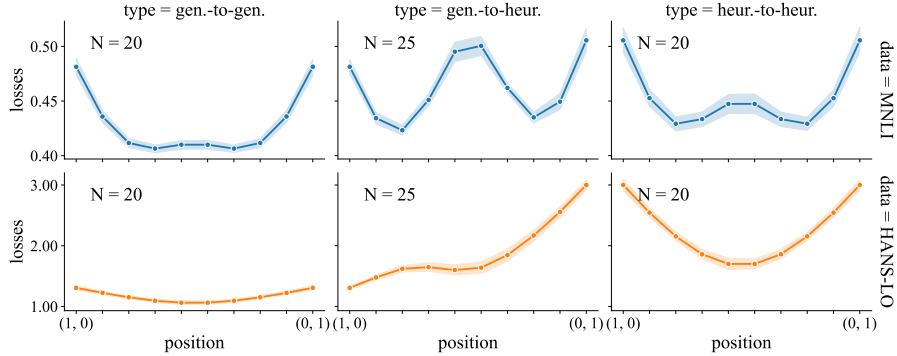
Frankle et al. [9] tested linear mode connectivity between models initialized from a single pruned network. They found that the resulting models achieved the same performance as the entire un-pruned network only when they were linearly connected. This result suggests that generalization, or at least high performance, is closely tied to the linear mode connectivity of the models in question. This implied result is further supported by Entezari et al. [7], which found a larger barrier between models when they exhibited higher test error. Neyshabur et al. [35] even described linear mode connectivity as a crucial component of transfer learning, finding that finetuned models initialized from the same pretrained model will be in the same linearly connected basin, in contrast to models trained from scratch, which exhibit barriers even when initialized from the same random weights.

Our results complicate the narrative around linear mode connectivity (Fig. 1(a)). While we find that models with high performance on OOD data were indeed linearly connected to each other, models with low performance were also linearly connected to each other. It seems that the heuristic and generalizing models occupy two different linear basins, with barriers in the ID loss surface between models in each of these two basins.

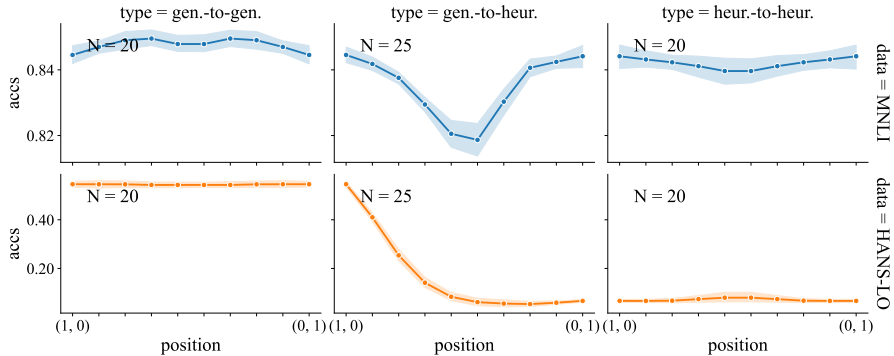
HANS performance during interpolation: It is clear from Fig. 1(a) that, when interpolating between LO-heuristic models, HANS-LO loss significantly improves further from the end points. This finding implies that the heuristic basin does contain more syntax-aware models. In contrast,

²https://storage.googleapis.com/bert_models/2018_10_18/uncased_L-12_H-768_A-12.zip

³<https://github.com/google-research/bert>



(a) MNLi and HANS-LO loss variation during linear interpolation.



(b) MNLi and HANS-LO accuracy variation during linear interpolation.

Figure 1: Performance during linear interpolation between pairs of models taken from the 5 top (gen.) and 5 bottom (heur.) in HANS-LO accuracy. Heuristic models tend to be poorly connected to the rest of the surface, although they are well connected to each other. N indicates number of pairs. Position on the x-axis indicates the value of α during interpolation.

the syntax-aware basin shows only a slight improvement in heuristic loss during interpolation, even though the improvement in ID test loss is more substantial than in the position-unaware basin. However, we can see from Fig. 1(b) that low losses on interpolated models do not always translate to consistently higher accuracy, although interpolated models that fall on barriers of elevated test loss do lead to lower ID accuracy.

Connections over 2 dimensions: To understand the loss topography better, we present planar views of these models using code⁴ from Benton et al. [1]. We see how, in the plane covering the heuristic and generalizing models, a central barrier intrudes on the linear connecting edge between heuristic and generalizing models (Fig. 2). On the other hand, the heuristic and generalizing models each occupy separate planes that exhibit only a small central barrier. Visibly, this barrier is smallest for the perimeter composed of generalizing models and largest for the mixed perimeter. These topographies motivate the following notion of an ϵ -convex basin.

3.1 Convex basins

Inspired by Entezari et al. [7], we define our notion of a basin in order to formalize types of behavior during linear interpolation. In contrast to their work, however, our goal is not to identify a largely stable region (the bottom of a basin). Instead, we are interested in whether a set of models are connected to the same low-loss points by a linear path of non-increasing loss. This motivation yields the following definition.

⁴<https://github.com/g-benton/loss-surface-simplexes>

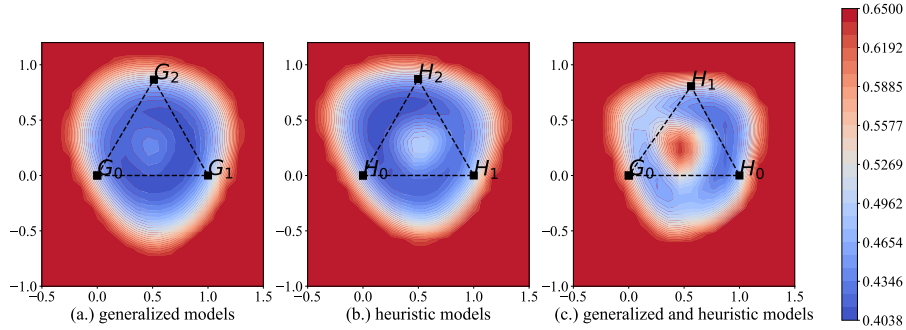


Figure 2: Planar views of simplices connecting NLI models in the MNLI matched validation set loss surface. The points $G_{0\dots 2}$ and $H_{0\dots 2}$ denote the generalizing and heuristic models respectively.

For resolution $\epsilon \geq 0$, we define an ϵ -convex basin as a convex set S , such that, for any set of points $w_1, w_2, \dots, w_k \in S$ and any set of coefficients $\alpha_1 \dots \alpha_n \geq 0$ where $\sum_k \alpha_k = 1$, a relaxed form of Jensen’s inequality holds:

$$\mathcal{L}\left(\sum_{k=1}^n \alpha_k w_k\right) \leq \epsilon + \sum_{k=1}^n \alpha_k \mathcal{L}(w_k) \quad (2)$$

In particular, we say that a set of trained models $\theta_1, \dots, \theta_n$ form an ϵ -convex basin if the region inside their convex hull is an ϵ -convex basin. In the case where $\epsilon = 0$, we can equivalently claim that the behavior of \mathcal{L} in the region is convex.

This definition satisfies our stated motivation because any two points within an ϵ -convex basin are connected linearly with monotonically (within ϵ) decaying loss to the same minima within that basin. While such a linear path does not strictly describe a typical SGD optimization trajectory, such linear interpolations are frequently used to analyze optimization behaviors like module criticality [35, 2]. One justification of this practice is that much of the oscillation and complexity of the training trajectory is constrained to short directions of the solution manifold [19, 53, 30], while large scale views of the landscape describe smoother and more linear trajectories [12, 8]. In this paper, we use this definition of ϵ -convexity to describe linearly connected points as existing in the same basin. However, pairwise non-increasing linear connections are a necessary but not sufficient condition for all convex combinations to be non-increasing, with counterexamples in Fig. 2.

4 The Convexity Gap

One possibility we argue against is that the increasing loss between models with different heuristics is actually an effect of sharper minima in the heuristic case. There is a significant body of work on the controversial [5] association between wider minima and generalization in models [26, 21, 17]. Prior work shows that minima forced to memorize a training set without generalizing on a test set exist in very sharp basins [18], but these basins are discovered only by directly pessimizing on the test set. It is less clear whether width is predictive of generalization across models trained conventionally.

On the contrary, we find that clusters of linearly connected models are far better predictors of generalization behavior than optimum width is. To identify such clusters, we define a metric based on linear mode connectivity, the **convexity gap** ($\mathcal{C}\mathcal{G}$), and use it to perform spectral clustering.

Entezari et al. [7] define a barrier’s height on a linear path from θ_1 to θ_2 as:

$$\mathfrak{B}\mathfrak{H}(\theta_1, \theta_2) = \sup_{\alpha} [\mathcal{L}(\alpha\theta_1 + (1 - \alpha)\theta_2) - (\alpha\mathcal{L}(\theta_1) + (1 - \alpha)\mathcal{L}(\theta_2))] \quad \alpha \in [0, 1] \quad (3)$$

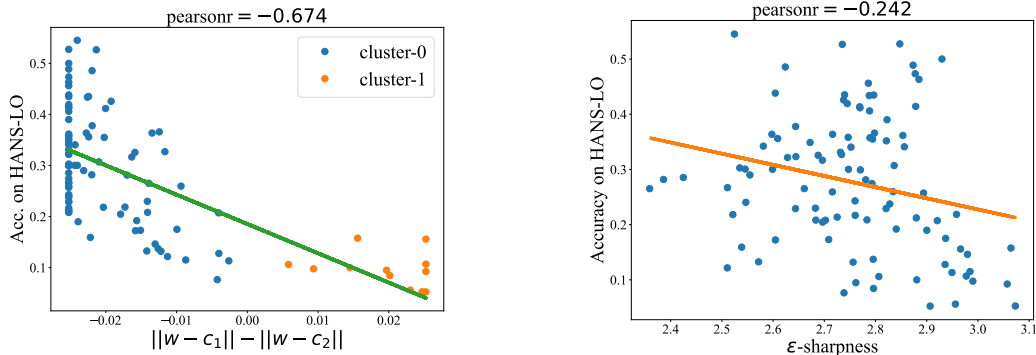


Figure 3: Using features of the ID loss landscape to predict reliance on lexical overlap heuristics. Least squares fit shown. (a) HANS-LO performance vs difference between distances from the centroids c_1, c_2 of the $\mathcal{C}\mathcal{G}$ -based clusters. (b) HANS-LO performance vs ϵ -sharpness.

We define the convexity gap on a linear path from θ_1 to θ_2 as the maximum possible barrier height on any sub-segment of the linear path joining θ_1 and θ_2 . Mathematically,

$$\mathcal{C}\mathcal{G}(\theta_1, \theta_2) = \sup_{\gamma, \beta} \mathfrak{B}\mathfrak{H}(\gamma\theta_1 + (1 - \gamma)\theta_2, \beta\theta_1 + (1 - \beta)\theta_2) \quad \gamma, \beta \in [0, 1] \quad (4)$$

Under this definition, an ϵ -convex basin has a convexity gap of at most ϵ within the basin (proof in Appendix B). Our metric exposes stronger clustering patterns than either area under the curve (AUC) or $\mathfrak{B}\mathfrak{H}$ (evidence in Appendix I).

4.1 Clustering

The basins that form from this distance metric are visible based on connected sets of models in the distance heatmap (Fig. 4(a)). To quantify basin membership into a prediction of HANS performance, we perform spectral clustering, with the distances between points defined as $\mathcal{C}\mathcal{G}$ -distance on the ID loss surface. Using the difference between distances from each cluster centroid $\|w - c_1\|$ and $\|w - c_2\|$, we see a significantly larger correlation with HANS performance (Fig. 3(a)), compared to a baseline of the model’s ϵ -sharpness (Fig. 3(b)). Furthermore, a linear regression model offers significantly better performance based on spectral clustering membership than sharpness.⁵

In Fig. 4(b), we see the heuristic that defines the larger cluster: constituent overlap. Models that perform well on constituent overlap diagnostic sets tend to fall in the basin containing models biased towards lexical overlap. This behavior characterizes the two basins: the larger basin is syntax-aware (tending to acquire heuristics that require awareness of constituent structure), while the smaller basin is syntax-unaware (acquiring heuristics that rely only on unordered sets of words).⁶

Distributions of the clusters: We find (Fig. 5) that $\mathcal{C}\mathcal{G}$ -based cluster membership accounts for some of the heavy tail of performance on HANS-LO, supporting the claim that the convex basins on the loss surface differentiate generalization strategies. However, the distribution of ID performance also differs significantly between clusters, so we may choose to relate basin membership to ID behavior instead of OOD. We discuss this alternative framing further in Appendix H.

⁵The connection between cluster membership and generalization performance is continuous. That is, those members of the syntax-aware cluster which are closer to the cluster boundary behave a little more like bag-of-words models, rather than behaving like typical syntax-aware models. The existence of marginally syntax-aware models is unsurprising; we already know that there are models in the heuristic basin that are slightly more syntax-aware, because they are visible at midpoints during interpolation between heuristic models (Fig. 1(a)).

⁶It is not enough to declare one basin to be merely *position* aware, as reliance on subsequence overlap is a poor predictor of basin membership (Appendix C).

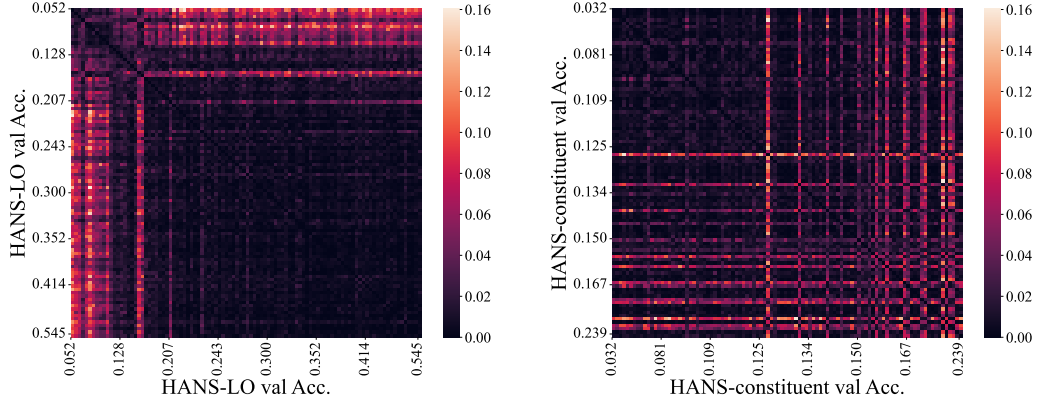


Figure 4: Color indicates $\mathcal{C}\mathcal{E}$ distance between the x- and y-axis NLI models. (a) Models sorted by increasing performance on HANS-LO. (b) Sorted by increasing performance on HANS-constituent.

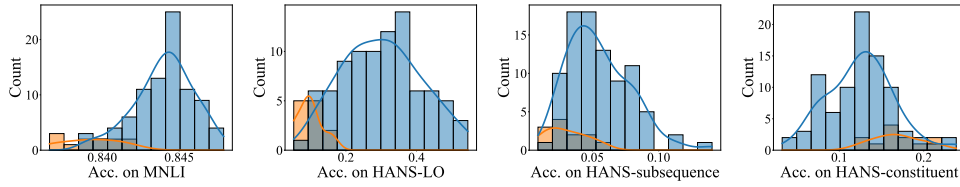


Figure 5: Histogram of accuracy scores of the different NLI clusters.

4.1.1 QQP

On QQP, we similarly find strong differentiation between distinct clusters of linearly connected models (Fig. 6(a)). As in our procedure on NLI, we study the distance from the centroids formed by spectral clustering with $\mathcal{C}\mathcal{E}$ defining the distance metric, and find cluster membership to be a strong predictor of generalization on PAWS-QQP (Fig. 6(b)).

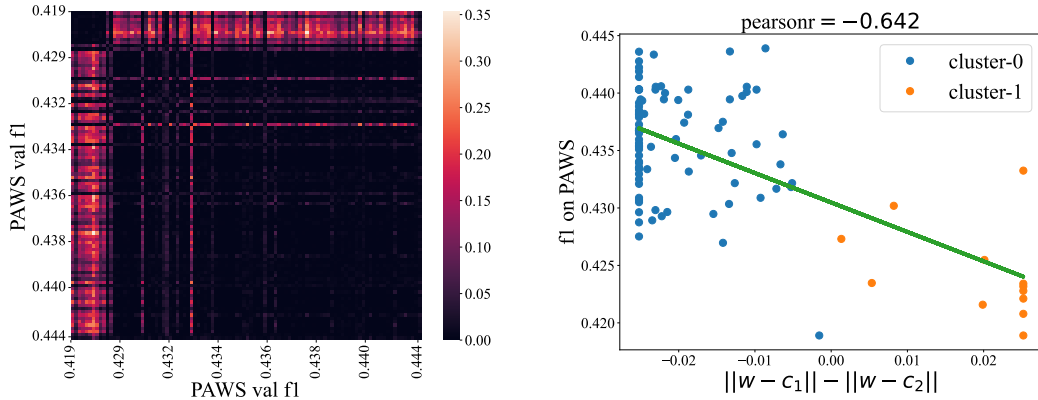


Figure 6: (a) $\mathcal{C}\mathcal{E}$ heatmap with QQP models sorted according to f1 score on PAWS-QQP. (b) QQP cluster membership is highly predictive of PAWS-QQP performance. Least squares fit shown.

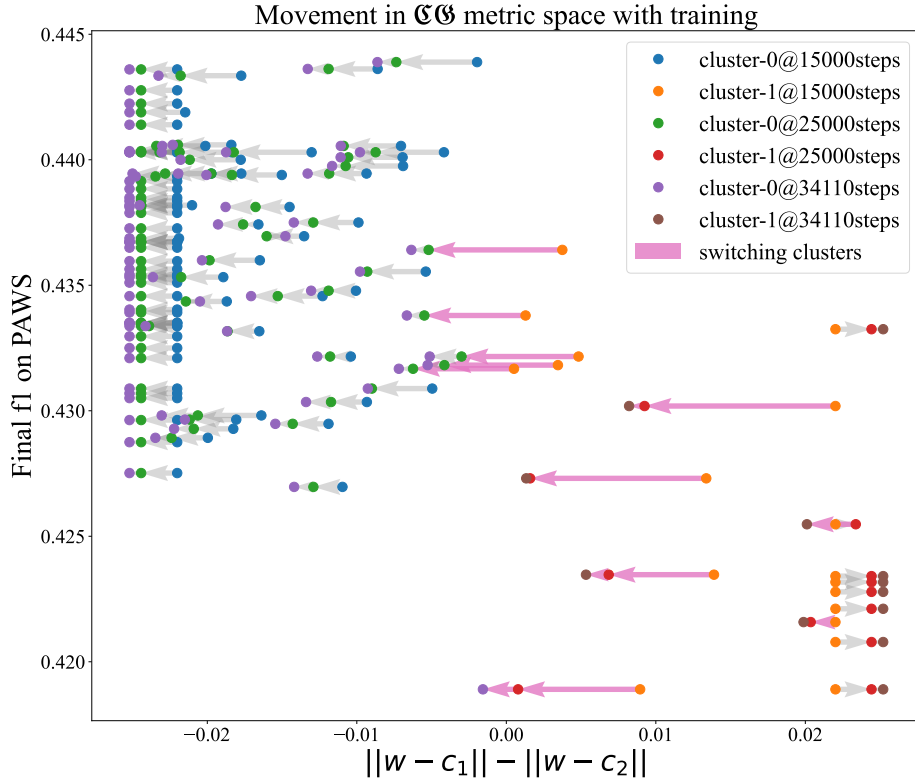


Figure 7: Movement between clusters during finetuning. Syntax-unaware models near the cluster boundary move towards the syntax-aware cluster, but central models in both clusters move closer to their respective centroids.

4.2 Generalization basins trap training trajectories

At this point we have aligned different basins with particular generalization behaviors, but a skeptic may propose that the smaller cluster contains models which have simply not trained long enough. Under this conjecture, continuing to train them would eventually place them in the larger, syntax-aware cluster. We find that this is not the case, as shown in Fig. 7. Marginal members of the smaller cluster, those which fall closer to the cluster boundary, may drift towards the larger cluster later in training. However, models that are more central to the cluster actually become increasingly solidified in their cluster membership later in training.

These results have two important implications. First, they confirm that these basins constitute distinct local minima which can trap optimization trajectories. Additionally, our findings suggest that early on in training, we can detect whether a final model will follow a particular heuristic. The latter conclusion is crucial for any future work towards practical methods of directing or detecting desirable generalization strategies during training [20].

5 Related Work

Connectivity of the Loss Landscape: Draxler et al. [6] demonstrated that pairs of trained models are generally connected to each other by nonlinear paths of constant train and test loss. Garipov et al. [10] and Fort and Jastrzebski [8] conceptualized these paths as high dimensional volumes connecting entire sets of solutions. Goodfellow et al. [12] explored linear connections between model pairs by interpolating between them, while [7] suggested that in general, models that seem linearly disconnected may be connected after permuting their neurons. Our work explores models that are linearly connected without permutation, and is most closely linked with Neyshabur et al. [35], which found that models initialized from a shared pretrained checkpoint are linearly connected. Frankle

et al. [9] also found that pruned initial weights can lead to trained models that interpolate with low loss, if the pruned model generalizes well. These results, unlike ours, focus on image classification.

Generalization: Diagnostic challenge sets are a common method for evaluating generalization behavior in a number of modalities. Imagenet has a number of corresponding diagnostic sets, from naturally-hard examples [25, 15] to perturbed images [14] to sketched renderings of objects [46]. In NLP, diagnostic sets frequently focus on compositionality and grammatical behavior such as inflection agreement [24, 41]. Diagnostic sets in NLP can be based on natural adversarial data [13, 27], constructed by perturbations and rephrases [39, 11], or generated artificially from templates [38, 55]. NLI models in particular often fail on diagnostic sets with permuted word order [22, 34, 32], often exposing a lack of syntactic behavior. Our case study is particularly informative because interpretability of NLI datasets reveals classes of generalization strategies.

Function Diversity: Initializing from a single pretrained model can produce a range of in-domain generalization behaviors [4, 36, 40, 33]. However, variation on performance in diagnostic sets is even more substantial, from social biases [40] to unusual paraphrases [31, 56]. Benton et al. [1] found that a wide variety of decision boundaries were expressed within a low-loss volume, and Somepalli et al. [43] further found that there is diversity in boundaries during OOD generalization, far off the data manifold. Our work contributes to diversity in generalization by linking sets of models that share low dimensional subspaces to particular OOD generalization behavior. We also expand beyond visualizing decision boundaries by focusing on the geography of basins aligned with specific interpretable strategies, particularly syntax-aware heuristics.

6 Discussion and Future Work

Future research may focus on evaluating the strength and nature of the prior distribution over basins. Transfer learning priors range from the high entropy distribution provided by training from scratch to those pretrained models which seem to consistently select a single basin [35]. Possible influences on basin selection, and therefore on generalization strategies, may include length of pretraining [49], data scheduling, and architecture selection [43]. The strength of a prior towards particular basins may be not only linked to training procedure, but also strongly related to the availability of features in the pretrained representations [29, 16, 42]. This aspect of transfer learning is a particularly ripe area for theoretical work in optimization.

Another possible direction for future work is to identify early on whether a basin has a desirable generalization strategy. For example, can we detect early on if a Transformer model is unable to use position information, instead acting as a bag of words? It is particularly promising that $\mathcal{L}_{\mathcal{G}}$ in training loss is highly predictive of OOD generalization even without any validation set (Appendix G), so the only investigation needed is of the loss surface during training. Furthermore, a model tends to stay in the same cluster in early and late training (Section 4.2), so final heuristics should be easy to predict from earlier basin membership.

The split between generalization strategies can potentially explain results from the bimodality of CoLA models [33] to wide variance on NLI diagnostic sets [31]. Because weight averaging can find parameter settings that fall on a barrier, we may even explain why weight averaging, which tends to perform well on vision tasks, fails in text classifiers [52]. Future work that distinguishes generalization strategy basins could improve the performance of such weight ensembling methods.

Because these methods rely on a high likelihood of linear mode connectivity, they are particular to transfer learning [35] or other settings with a similar connectivity bias [9]. We could also study pretrained models themselves or training from scratch, but only if we first align the neurons [7, 44] so that the vectors being averaged match in their role within the function space.

Within NLP, many tasks and accompanying generalization strategies can be further explored. There are general tests of inductive bias towards grammatical behavior [49], as well as other diagnostic sets. Outside of text classification, sequence-to-sequence tasks provide a number of possible tests for generalization behavior. For language modeling itself, we can consider biases towards subject-verb number agreement or other ways of matching inflection [27, 13, 37]. OOD generalization tests are also available for seq2seq tasks like semantic parsing [23].

While we focus on text classification due to the availability of diagnostic datasets that test structural generalization, other modalities such as vision may have distinct generalization strategies. In some domain shift scenarios [25, 46, 15, 14], OOD generalization behavior may therefore form basins. In current work, however, barriers are not observed in vision during transfer [35, 52]. Is that because *all* vision models achieve a basin with good structural generalization—or none do?

7 Conclusions

In one view of transfer learning, a pretrained model may select a prior over generalization strategies by favoring a particular basin. Neyshabur et al. [35] found that models initialized from the same pretrained weights are linearly connected, suggesting that basin selection is a key component of transfer learning. We find that a pretrained model may not commit exclusively to a single basin, but instead favor a small set of them. Furthermore, we find that linear connectivity can indicate shared generalization strategies under domain shift, as evidenced by results on NLI, paraphrase, and linguistic acceptability tasks.

References

- [1] G. W. Benton, W. J. Maddox, S. Lotfi, and A. G. Wilson. Loss Surface Simplexes for Mode Connecting Volumes and Fast Ensembling. *arXiv:2102.13042 [cs, stat]*, Feb. 2021. URL <http://arxiv.org/abs/2102.13042>. arXiv: 2102.13042.
- [2] N. Chatterji, B. Neyshabur, and H. Sedghi. The intriguing role of module criticality in the generalization of deep networks. In *International Conference on Learning Representations*, 2020. URL <https://openreview.net/forum?id=S1e4jkSKvB>.
- [3] T. F. Consortium, R. Cooper, D. Crouch, J. V. Eijck, C. Fox, J. V. Genabith, J. Jaspars, H. Kamp, D. Milward, M. Pinkal, M. Poesio, S. Pulman, T. Briscoe, H. Maier, and K. Konrad. Using the framework, 1996.
- [4] J. Devlin, M.-W. Chang, K. Lee, and K. Toutanova. Bert: Pre-training of deep bidirectional transformers for language understanding. *ArXiv*, abs/1810.04805, 2019.
- [5] L. Dinh, R. Pascanu, S. Bengio, and Y. Bengio. Sharp Minima Can Generalize For Deep Nets. *arXiv:1703.04933 [cs]*, May 2017. URL <http://arxiv.org/abs/1703.04933>. arXiv: 1703.04933.
- [6] F. Draxler, K. Veschgini, M. Salmhofer, and F. A. Hamprecht. Essentially No Barriers in Neural Network Energy Landscape. *arXiv:1803.00885 [cs, stat]*, Feb. 2019. URL <http://arxiv.org/abs/1803.00885>. arXiv: 1803.00885.
- [7] R. Entezari, H. Sedghi, O. Saukh, and B. Neyshabur. The Role of Permutation Invariance in Linear Mode Connectivity of Neural Networks. *arXiv:2110.06296 [cs]*, Oct. 2021. URL <http://arxiv.org/abs/2110.06296>. arXiv: 2110.06296.
- [8] S. Fort and S. Jastrzebski. Large Scale Structure of Neural Network Loss Landscapes. In *Advances in Neural Information Processing Systems*, volume 32. Curran Associates, Inc., 2019. URL <https://proceedings.neurips.cc/paper/2019/hash/48042b1dae4950fef2bd2aafa0b971a1-Abstract.html>.
- [9] J. Frankle, G. K. Dziugaite, D. Roy, and M. Carbin. Linear Mode Connectivity and the Lottery Ticket Hypothesis. In *Proceedings of the 37th International Conference on Machine Learning*, pages 3259–3269. PMLR, Nov. 2020. URL <https://proceedings.mlr.press/v119/frankle20a.html>. ISSN: 2640-3498.
- [10] T. Garipov, P. Izmailov, D. Podoprikin, D. Vetrov, and A. G. Wilson. Loss Surfaces, Mode Connectivity, and Fast Ensembling of DNNs. *arXiv:1802.10026 [cs, stat]*, Oct. 2018. URL <http://arxiv.org/abs/1802.10026>. arXiv: 1802.10026.
- [11] M. Glockner, V. Shwartz, and Y. Goldberg. Breaking NLI systems with sentences that require simple lexical inferences. In *Proceedings of the 56th Annual Meeting of the Association for Computational Linguistics (Volume 2: Short Papers)*, pages 650–655, Melbourne, Australia, July 2018. Association for Computational Linguistics. doi: 10.18653/v1/P18-2103. URL <https://aclanthology.org/P18-2103>.

- [12] I. J. Goodfellow, O. Vinyals, and A. M. Saxe. Qualitatively characterizing neural network optimization problems. *arXiv:1412.6544 [cs, stat]*, May 2015. URL <http://arxiv.org/abs/1412.6544>. arXiv: 1412.6544.
- [13] K. Gulordava, P. Bojanowski, E. Grave, T. Linzen, and M. Baroni. Colorless green recurrent networks dream hierarchically. *arXiv:1803.11138 [cs]*, Mar. 2018. URL <http://arxiv.org/abs/1803.11138>. arXiv: 1803.11138.
- [14] D. Hendrycks and T. Dietterich. Benchmarking neural network robustness to common corruptions and perturbations. *Proceedings of the International Conference on Learning Representations*, 2019.
- [15] D. Hendrycks, K. Zhao, S. Basart, J. Steinhardt, and D. Song. Natural adversarial examples. *CVPR*, 2021.
- [16] K. L. Hermann and A. K. Lampinen. What shapes feature representations? Exploring datasets, architectures, and training. *arXiv:2006.12433 [cs, stat]*, Oct. 2020. URL <http://arxiv.org/abs/2006.12433>. arXiv: 2006.12433.
- [17] S. Hochreiter and J. Schmidhuber. Flat minima. *Neural Computation*, 9:1–42, 1997.
- [18] W. R. Huang, Z. Emam, M. Goldblum, L. Fowl, J. K. Terry, F. Huang, and T. Goldstein. Understanding Generalization through Visualizations. *arXiv:1906.03291 [cs, stat]*, Nov. 2020. URL <http://arxiv.org/abs/1906.03291>. arXiv: 1906.03291.
- [19] S. Jastrzebski, M. Szymczak, S. Fort, D. Arpit, J. Tabor, K. Cho, and K. Geras. The Break-Even Point on Optimization Trajectories of Deep Neural Networks. *arXiv:2002.09572 [cs, stat]*, Feb. 2020. URL <http://arxiv.org/abs/2002.09572>. arXiv: 2002.09572.
- [20] S. Jastrzebski, D. Arpit, O. Astrand, G. B. Kerg, H. Wang, C. Xiong, R. Socher, K. Cho, and K. J. Geras. Catastrophic Fisher Explosion: Early Phase Fisher Matrix Impacts Generalization. In *Proceedings of the 38th International Conference on Machine Learning*, pages 4772–4784. PMLR, July 2021. URL <https://proceedings.mlr.press/v139/jastrzebski21a.html>. ISSN: 2640-3498.
- [21] N. S. Keskar, D. Mudigere, J. Nocedal, M. Smelyanskiy, and P. T. P. Tang. On large-batch training for deep learning: Generalization gap and sharp minima. *ArXiv*, abs/1609.04836, 2017.
- [22] J. Kim, C. Malon, and A. Kadav. Teaching syntax by adversarial distraction. In *Proceedings of the First Workshop on Fact Extraction and VERification (FEVER)*, pages 79–84, Brussels, Belgium, Nov. 2018. Association for Computational Linguistics. doi: 10.18653/v1/W18-5512. URL <https://aclanthology.org/W18-5512>.
- [23] N. Kim and T. Linzen. COGS: A Compositional Generalization Challenge Based on Semantic Interpretation. In *Proceedings of the 2020 Conference on Empirical Methods in Natural Language Processing (EMNLP)*, pages 9087–9105, Online, Nov. 2020. Association for Computational Linguistics. doi: 10.18653/v1/2020.emnlp-main.731. URL <https://aclanthology.org/2020.emnlp-main.731>.
- [24] N. Kim, R. Patel, A. Poliak, P. Xia, A. Wang, T. McCoy, I. Tenney, A. Ross, T. Linzen, B. Van Durme, S. R. Bowman, and E. Pavlick. Probing what different NLP tasks teach machines about function word comprehension. In *Proceedings of the Eighth Joint Conference on Lexical and Computational Semantics (*SEM 2019)*, pages 235–249, Minneapolis, Minnesota, June 2019. Association for Computational Linguistics. doi: 10.18653/v1/S19-1026. URL <https://aclanthology.org/S19-1026>.
- [25] P. W. Koh, S. Sagawa, H. Marklund, S. M. Xie, M. Zhang, A. Balsubramani, W. Hu, M. Yasunaga, R. L. Phillips, I. Gao, T. Lee, E. David, I. Stavness, W. Guo, B. A. Earnshaw, I. S. Haque, S. Beery, J. Leskovec, A. Kundaje, E. Pierson, S. Levine, C. Finn, and P. Liang. WILDS: A Benchmark of in-the-Wild Distribution Shifts. *arXiv:2012.07421 [cs]*, July 2021. URL <http://arxiv.org/abs/2012.07421>. arXiv: 2012.07421.
- [26] H. Li, Z. Xu, G. Taylor, C. Studer, and T. Goldstein. Visualizing the Loss Landscape of Neural Nets. In S. Bengio, H. Wallach, H. Larochelle, K. Grauman, N. Cesa-Bianchi, and R. Garnett, editors, *Advances in Neural Information Processing Systems 31*, pages 6389–6399. Curran Associates, Inc., 2018. URL <http://papers.nips.cc/paper/7875-visualizing-the-loss-landscape-of-neural-nets.pdf>.

- [27] T. Linzen, E. Dupoux, and Y. Goldberg. Assessing the Ability of LSTMs to Learn Syntax-Sensitive Dependencies. *arXiv:1611.01368 [cs]*, Nov. 2016. URL <http://arxiv.org/abs/1611.01368>. arXiv: 1611.01368.
- [28] I. Loshchilov and F. Hutter. Decoupled weight decay regularization, 2017. URL <https://arxiv.org/abs/1711.05101>.
- [29] C. Lovering, R. Jha, T. Linzen, and E. Pavlick. Predicting inductive biases of pre-trained models. In *ICLR*, 2021.
- [30] C. Ma, L. Wu, and L. Ying. The Multiscale Structure of Neural Network Loss Functions: The Effect on Optimization and Origin. *arXiv:2204.11326 [cs]*, Apr. 2022. URL <http://arxiv.org/abs/2204.11326>. arXiv: 2204.11326.
- [31] R. T. McCoy, J. Min, and T. Linzen. Berts of a feather do not generalize together: Large variability in generalization across models with similar test set performance. *ArXiv*, abs/1911.02969, 2020.
- [32] T. McCoy, E. Pavlick, and T. Linzen. Right for the Wrong Reasons: Diagnosing Syntactic Heuristics in Natural Language Inference. In *Proceedings of the 57th Annual Meeting of the Association for Computational Linguistics*, pages 3428–3448, Florence, Italy, July 2019. Association for Computational Linguistics. doi: 10.18653/v1/P19-1334. URL <https://aclanthology.org/P19-1334>.
- [33] M. Mosbach, M. Andriushchenko, and D. Klakow. On the Stability of Fine-tuning BERT: Misconceptions, Explanations, and Strong Baselines. *arXiv:2006.04884 [cs, stat]*, Mar. 2021. URL <http://arxiv.org/abs/2006.04884>. arXiv: 2006.04884.
- [34] A. Naik, A. Ravichander, N. Sadeh, C. Rose, and G. Neubig. Stress test evaluation for natural language inference. In *Proceedings of the 27th International Conference on Computational Linguistics*, pages 2340–2353, Santa Fe, New Mexico, USA, Aug. 2018. Association for Computational Linguistics. URL <https://aclanthology.org/C18-1198>.
- [35] B. Neyshabur, H. Sedghi, and C. Zhang. What is being transferred in transfer learning? In *Advances in Neural Information Processing Systems*, volume 33, pages 512–523. Curran Associates, Inc., 2020. URL <https://papers.nips.cc/paper/2020/hash/0607f4c705595b911a4f3e7a127b44e0-Abstract.html>.
- [36] J. Phang, J. Park, and K. J. Geras. Investigating and Simplifying Masking-based Saliency Methods for Model Interpretability. *arXiv:2010.09750 [cs]*, Oct. 2020. URL <http://arxiv.org/abs/2010.09750>. arXiv: 2010.09750.
- [37] S. Ravfogel, Y. Goldberg, and T. Linzen. Studying the Inductive Biases of RNNs with Synthetic Variations of Natural Languages. *arXiv:1903.06400 [cs]*, Mar. 2019. URL <http://arxiv.org/abs/1903.06400>. arXiv: 1903.06400.
- [38] R. Rudinger, J. Naradowsky, B. Leonard, and B. Van Durme. Gender bias in coreference resolution. In *Proceedings of the 2018 Conference of the North American Chapter of the Association for Computational Linguistics: Human Language Technologies, Volume 2 (Short Papers)*, pages 8–14, New Orleans, Louisiana, June 2018. Association for Computational Linguistics. doi: 10.18653/v1/N18-2002. URL <https://aclanthology.org/N18-2002>.
- [39] I. Sanchez, J. Mitchell, and S. Riedel. Behavior analysis of NLI models: Uncovering the influence of three factors on robustness. In *Proceedings of the 2018 Conference of the North American Chapter of the Association for Computational Linguistics: Human Language Technologies, Volume 1 (Long Papers)*, pages 1975–1985, New Orleans, Louisiana, June 2018. Association for Computational Linguistics. doi: 10.18653/v1/N18-1179. URL <https://aclanthology.org/N18-1179>.
- [40] T. Sellam, S. Yadlowsky, I. Tenney, J. Wei, N. Saphra, A. D’Amour, T. Linzen, J. Bastings, I. R. Turc, J. Eisenstein, D. Das, and E. Pavlick. The MultiBERTs: BERT Reproductions for Robustness Analysis. In *ICLR*, Sept. 2021. URL https://openreview.net/forum?id=KOE_F0gFDgA.
- [41] R. Sennrich. How grammatical is character-level neural machine translation? assessing MT quality with contrastive translation pairs. In *Proceedings of the 15th Conference of the European Chapter of the Association for Computational Linguistics: Volume 2, Short Papers*, pages 376–382, Valencia, Spain, Apr. 2017. Association for Computational Linguistics. URL <https://aclanthology.org/E17-2060>.

- [42] H. Shah, K. Tamuly, A. Raghunathan, P. Jain, and P. Netrapalli. The Pitfalls of Simplicity Bias in Neural Networks. *arXiv:2006.07710 [cs, stat]*, Oct. 2020. URL <http://arxiv.org/abs/2006.07710>. arXiv: 2006.07710.
- [43] G. Somepalli, L. Fowl, A. Bansal, P. Yeh-Chiang, Y. Dar, R. Baraniuk, M. Goldblum, and T. Goldstein. Can Neural Nets Learn the Same Model Twice? Investigating Reproducibility and Double Descent from the Decision Boundary Perspective. *arXiv:2203.08124 [cs]*, Mar. 2022. URL <http://arxiv.org/abs/2203.08124>. arXiv: 2203.08124.
- [44] N. J. Tatro, P.-Y. Chen, P. Das, I. Melnyk, P. Sattigeri, and R. Lai. Optimizing Mode Connectivity via Neuron Alignment. *arXiv:2009.02439 [cs, math, stat]*, Nov. 2020. URL <http://arxiv.org/abs/2009.02439>. arXiv: 2009.02439.
- [45] A. Wang, A. Singh, J. Michael, F. Hill, O. Levy, and S. R. Bowman. Glue: A multi-task benchmark and analysis platform for natural language understanding. *ArXiv*, abs/1804.07461, 2018.
- [46] H. Wang, S. Ge, Z. Lipton, and E. P. Xing. Learning robust global representations by penalizing local predictive power. In *Advances in Neural Information Processing Systems*, pages 10506–10518, 2019.
- [47] Z. Wang, W. Hamza, and R. Florian. Bilateral multi-perspective matching for natural language sentences. *ArXiv*, abs/1702.03814, 2017.
- [48] A. Warstadt, A. Singh, and S. R. Bowman. Neural network acceptability judgments. *arXiv preprint arXiv:1805.12471*, 2018.
- [49] A. Warstadt, Y. Zhang, X. Li, H. Liu, and S. R. Bowman. Learning Which Features Matter: RoBERTa Acquires a Preference for Linguistic Generalizations (Eventually). In *Proceedings of the 2020 Conference on Empirical Methods in Natural Language Processing (EMNLP)*, pages 217–235, Online, Nov. 2020. Association for Computational Linguistics. URL <https://www.aclweb.org/anthology/2020.emnlp-main.16>.
- [50] A. Williams, N. Nangia, and S. Bowman. A broad-coverage challenge corpus for sentence understanding through inference. In *Proceedings of the 2018 Conference of the North American Chapter of the Association for Computational Linguistics: Human Language Technologies, Volume 1 (Long Papers)*, pages 1112–1122. Association for Computational Linguistics, 2018. URL <http://aclweb.org/anthology/N18-1101>.
- [51] T. Wolf, L. Debut, V. Sanh, J. Chaumond, C. Delangue, A. Moi, P. Cistac, T. Rault, R. Louf, M. Funtowicz, J. Davison, S. Shleifer, P. von Platen, C. Ma, Y. Jernite, J. Plu, C. Xu, T. Le Scao, S. Gugger, M. Drame, Q. Lhoest, and A. Rush. Transformers: State-of-the-art natural language processing. In *Proceedings of the 2020 Conference on Empirical Methods in Natural Language Processing: System Demonstrations*, pages 38–45, Online, Oct. 2020. Association for Computational Linguistics. doi: 10.18653/v1/2020.emnlp-demos.6. URL <https://aclanthology.org/2020.emnlp-demos.6>.
- [52] M. Wortsman, G. Ilharco, S. Y. Gadre, R. Roelofs, R. Gontijo-Lopes, A. S. Morcos, H. Namkoong, A. Farhadi, Y. Carmon, S. Kornblith, and L. Schmidt. Model soups: averaging weights of multiple fine-tuned models improves accuracy without increasing inference time. *arXiv:2203.05482 [cs]*, Mar. 2022. URL <http://arxiv.org/abs/2203.05482>. arXiv: 2203.05482.
- [53] C. Xing, D. Arpit, C. Tsirigotis, and Y. Bengio. A Walk with SGD. *arXiv:1802.08770 [cs, stat]*, May 2018. URL <http://arxiv.org/abs/1802.08770>. arXiv: 1802.08770.
- [54] Y. Zhang, J. Baldridge, and L. He. PAWS: Paraphrase Adversaries from Word Scrambling. In *Proc. of NAACL*, 2019.
- [55] J. Zhao, T. Wang, M. Yatskar, V. Ordonez, and K.-W. Chang. Gender bias in coreference resolution: Evaluation and debiasing methods. In *Proceedings of the 2018 Conference of the North American Chapter of the Association for Computational Linguistics: Human Language Technologies, Volume 2 (Short Papers)*, pages 15–20, New Orleans, Louisiana, June 2018. Association for Computational Linguistics. doi: 10.18653/v1/N18-2003. URL <https://aclanthology.org/N18-2003>.
- [56] X. Zhou, Y. Nie, H. Tan, and M. Bansal. The Curse of Performance Instability in Analysis Datasets: Consequences, Source, and Suggestions. *arXiv:2004.13606 [cs]*, Nov. 2020. URL <http://arxiv.org/abs/2004.13606>. arXiv: 2004.13606.

A Linguistic Acceptability

The Corpus of Linguistic Acceptability [CoLA; 48] is a set of acceptable and unacceptable English sentences collected from the linguistics literature. Linguistics has a longstanding practice of studying minimal changes that render sentences ungrammatical; one CoLA example is the pair of sentences “Betsy buttered the toast” (acceptable) and “Betsy buttered at the toast” (unacceptable).

CoLA includes an ID val/test set, where the examples are taken from the same linguistics papers that the training set uses. However, it also includes an OOD diagnostic val/test set. The diagnostic sets are taken from a different set of linguistics papers, so in order for a model to perform well on CoLA-OOD, it must transfer a general ability to recognize unacceptable English sentences, rather than simply learning the set of acceptability rules described in the ID sources.

A.1 Experimental details

We found that default settings on the HuggingFace [51] training script⁷ resulted in more pronounced barriers between models, compared to the Google script we used for NLI and QQP. Because our goal is to study the relationship between barriers and generalization, we therefore chose to use Huggingface for our CoLA analysis. Like in our other experiments, we kept the default hyperparameters, which differ slightly from the Google script. The CoLA models were trained for 6 epochs with a learning rate of 2×10^{-5} , a batch size of 32 samples, and 0 weight decay. Both scripts use the AdamW[28] optimizer with a linear learning rate decay schedule and no warm-up.

A.2 Clustering

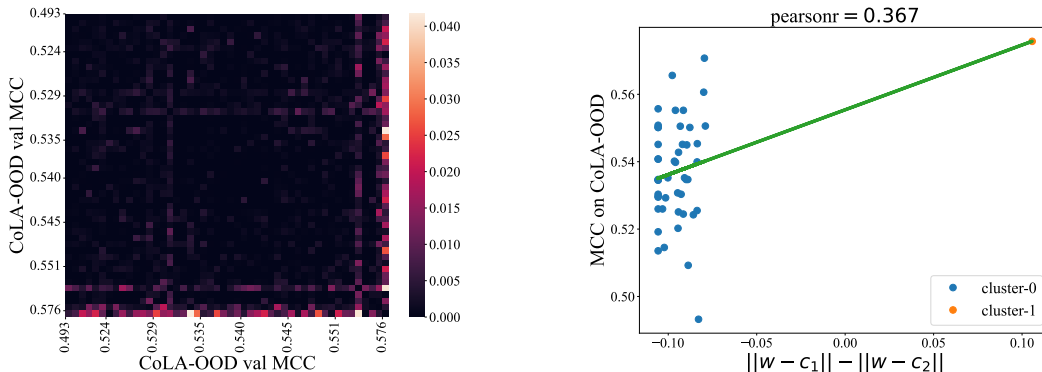


Figure 8: (a) \mathcal{CG} heatmap on CoLA models, sorted by OOD validation. (b) A scatter-plot of cluster membership versus performance on CoLA-OOD dev set.

In CoLA, there are very few barriers between finetuned models. A single model out of the 48 finetuned accounted for all substantial interpolation convexity gaps (Fig. 8(a)), thus forming its own one-point cluster when using \mathcal{CG} as a distance metric for spectral clustering. This outlier model outperformed all others on OOD generalization (Fig. 8(b)), suggesting that CoLA is another task where models with different generalization behavior are disconnected.

B Theoretical result on convexity gaps

Theorem 1. *An ϵ -basin will have $\mathcal{CG}(w_1, w_2) \leq \epsilon$ for every pair of models w_1, w_2 on its surface.*

Proof. Recall the definition of convexity gap as the maximum value of the barrier height of any segment θ_1, θ_2 along the interpolation between w_1 and w_2 from Equation 4:

$$\mathcal{CG}(w_1, w_2) = \sup_{\gamma, \beta} \mathfrak{B}\mathfrak{H}(\gamma w_1 + (1 - \gamma)w_2, \beta w_1 + (1 - \beta)w_2) \quad \gamma, \beta \in [0, 1] \quad (5)$$

⁷https://github.com/huggingface/transformers/blob/main/examples/flax/text-classification/run_flax_glue.py

As we are in an ϵ -basin, the defining inequality from Equation 2 holds $\forall \theta_1, \theta_2 \in \epsilon$ -convex basin :

$$\mathcal{L}\left(\sum_{k=1}^n \alpha_k \theta_k\right) \leq \epsilon + \sum_{k=1}^n \alpha_k \mathcal{L}(\theta_k) \quad (6)$$

Applying this for $n = 2$:

$$\mathcal{L}(\alpha_1 \theta_1 + (1 - \alpha_1) \theta_2) - (\alpha_1 \mathcal{L}(\theta_1) + (1 - \alpha_1) \mathcal{L}(\theta_2)) \leq \epsilon \quad \forall \theta_1, \theta_2 \in \epsilon\text{-basin} \quad (7)$$

Hence the supremum of the quantity on LHS is also $\leq \epsilon$. Seeing the definition of $\mathfrak{B}\mathfrak{H}$ from Equation 3, we immediately see that:

$$\mathfrak{B}\mathfrak{H}(\theta_1, \theta_2) \leq \epsilon \quad \forall \theta_1, \theta_2 \in \epsilon\text{-basin} \quad (8)$$

As $\mathcal{C}\mathcal{G}$ is the supremum of $\mathfrak{B}\mathfrak{H}$ over elements within the ϵ -convex basin only, we have:

$$\mathcal{C}\mathcal{G}(w_1, w_2) \leq \epsilon \quad \forall w_1, w_2 \in \epsilon\text{-basin} \quad (9)$$

□

C HANS performance on subsequence heuristics

Models that perform poorly on subsequence heuristics tend to fall in the bag-of-words basin. However, the clusters are less pronounced than for either constituent or lexical overlap heuristics (Fig. 9).

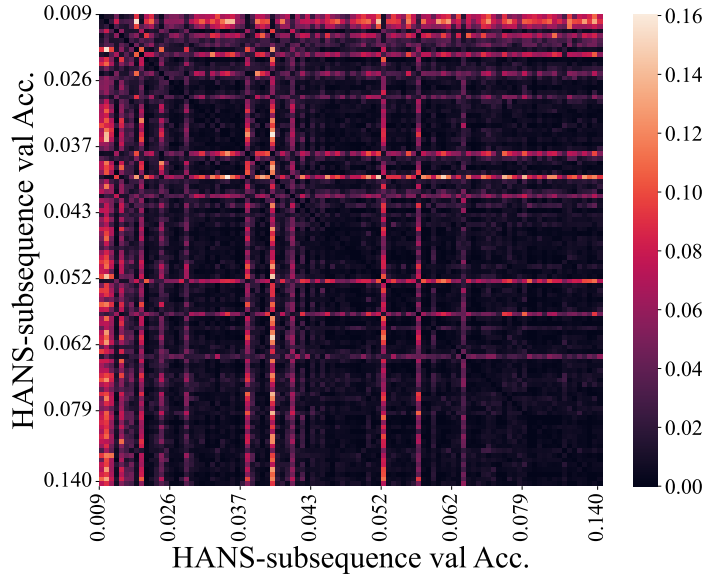


Figure 9: $\mathcal{C}\mathcal{G}$ for model pairs, sorted by increasing performance on HANS-subsequence.

D Flexible mode connectivity

While our results strongly suggest that linear mode connectivity breaks down between heuristic and generalizing models, they should nonetheless be connected, at least by a nonlinear path of constant training loss [6, 1]. We consider the behavior of HANS generalization along this path, which maintains near-constant ID loss. These paths were easy to identify with Riemannian curves and segmented lines [10], and exhibited poor HANS-LO generalization the further along the path the parameters fall, as shown in Fig. 10.

The results here show an inversion of the pattern exhibited on HANS-LO loss in the linear interpolation case: whereas Fig. 1(a) shows heuristic-to-generalizing connections to exhibit peaks in ID loss but no corresponding spikes in OOD loss, here we find constant-loss paths which exhibit peaks in HANS-LO loss. It appears that gradient descent finds generalizing models in spite of the fact that they exist in a constant-loss multidimensional volume which exhibits an apparent wealth of highly heuristic models.

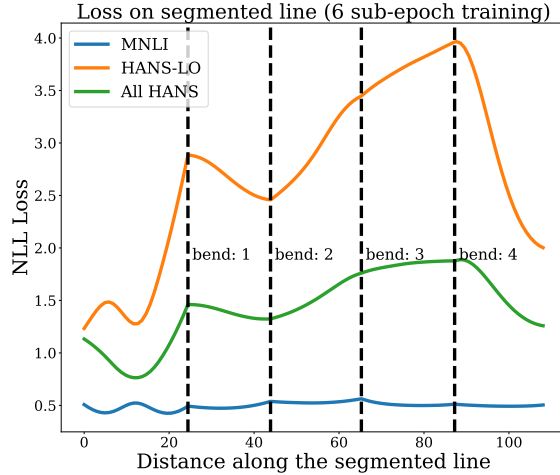


Figure 10: Loss along the segmented curve (after 6 subepochs) between a heuristic and generalizing NLI model. 1 sub-epoch is equivalent to ~ 120 training steps with a batch size of 128, and a learning rate of 8×10^{-5}

E Correlations between performance on HANS subsets

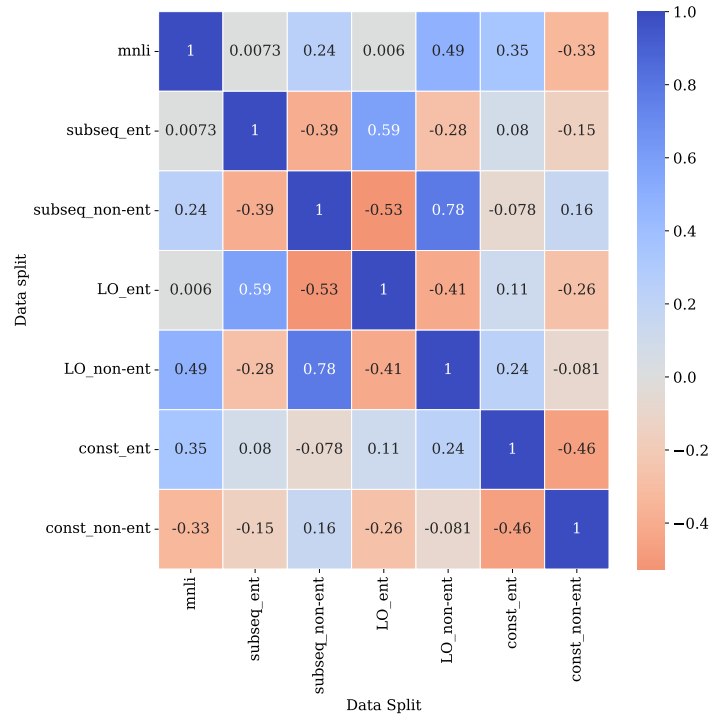


Figure 11: Correlation between accuracy on various ID and OOD diagnostic NLI test sets. MNLI refers to the MNLI validation set. Other sets were taken from HANS validation sets for subsequence, constituent, and lexical overlap heuristics. Both entailing and non-entailing subsets are included.

As provided in Fig. 11, performance on HANS-LO non-entailing, which reflects an aversion to the lexical overlap heuristic, is positively correlated with ID accuracy. However, in the case of HANS-constituent a model that successfully averts the constituent overlap heuristic is likely to perform poorly ID and on most diagnostic sets. We therefore conjecture that models which avoid

constituent overlap heuristics are likely failing to acquire syntax, rather than effectively acquiring better generalization strategies.

Performance on the subsequence heuristic diagnostic set is positively correlated with performance on both LO and constituent heuristic diagnostic sets, as it includes aspects of both other heuristics. For every diagnostic set heuristic, performance on the non-entailing subset (i.e., examples that violate the heuristic) is negatively correlated with performance on the entailing subset (i.e., examples that adhere to the heuristic).

F Experimental details

F.1 Finetuning the models

The QQP models were trained for 3 epochs, with a learning rate of 2×10^{-5} , a batch size of 32 samples and a weight decay of 0.01 from the `bert-base-uncased`⁸ pre-trained checkpoint using the `google` script.⁹ This script uses the AdamW [28] optimizer with a warm-up during the first 10% of the training followed by a linear schedule for weight decay. Because these hyperparameters are the recommended defaults for BERT training, they were also used by McCoy et al. [31] to train the MNLI model set we analyze.

F.2 Interpolations

In order to evaluate the interpolation between a pair of models, we sample a random set of 512 samples from the target dataset and then test each of the interpolated models on this same sample. For an interpolation between two fine-tuned models θ_1 and θ_2 , we evaluate the models with interpolation coefficients α at intervals of $\frac{1}{10}$ on the line joining θ_1 and θ_2 . The resulting plots are shown in Fig. 1(a) and Fig. 1(b). We calculate the convexity gap $\mathcal{CG}(\theta_1, \theta_2)$ is using the loss values of these interpolated models.

In order to gauge the effect of number of samples, we repeated interpolation experiments on MNLI using only 256 samples (instead of 512). Using a smaller sample reduced the magnitude of correlation coefficient in Fig. 3(a) to $\rho = -0.65$, but the cluster assignments remain the same.

F.3 Model Evaluations

When evaluating the performance of a finetuned model (e.g., to sort the models on the linear connectivity heatmaps, or to select the top and bottom 5 models for Fig. 1(a) and Fig. 1(b)), we use the whole dataset available. These include the entirety of:

- All non-entailing samples of a given heuristic from the `test` split of HANS.
- The `dev_and_test` split of PAWS-QQP.
- The entire QQP and MNLI validation sets.

As Feather-BERTs have been finetuned on MNLI, to evaluate them on HANS tasks, we would need to convert the logits for the three MNLI classes (`entailment`, `neutral`, `contradiction`) to logits for the two HANS classes (`entailing` and `non-entailing`). We convert these labels by taking the logit for non-entailing class as the maximum of the logits of the MNLI `contradiction` and `neutral` classes, and taking the logit for entailing class of HANS as the logit of entailing class of MNLI.

F.4 Computing sharpness

For calculating ϵ -sharpness of a model, we use the definition of Keskar et al. [21]:

$$\phi_{x,f}(\epsilon, A) := \frac{\max_{y \in \mathcal{C}_\epsilon} (f(x + Ay)) - f(x)}{1 + f(x)} \times 100 \quad (10)$$

⁸https://storage.googleapis.com/bert_models/2018_10_18/uncased_L-12_H-768_A-12.zip

⁹<https://github.com/google-research/bert>

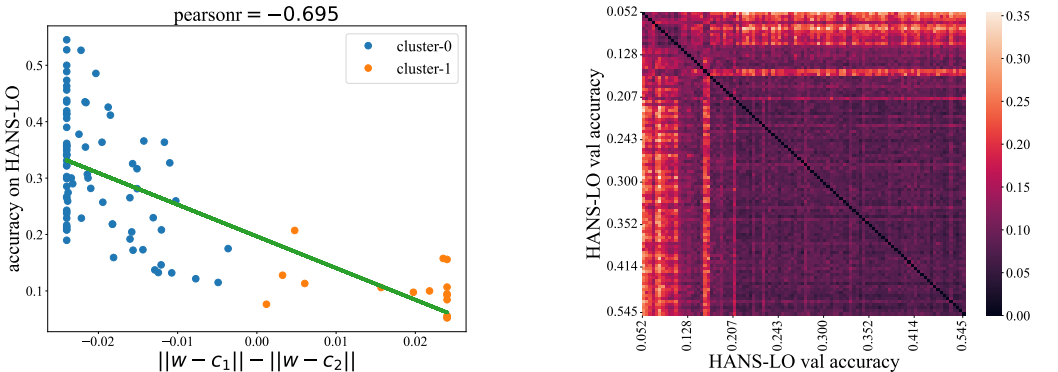
where f is the loss function, $x \in \mathbb{R}^n$ are the original parameters of the model, $A \in \mathbb{R}^{n \times p}$ is a matrix that restricts the calculation of ϵ -sharpness to a subspace of the parameter space, and

$$\mathcal{C}_\epsilon = \{z \in \mathbb{R}^p : -\epsilon(|(A^+x)_i| + 1) \leq z_i \leq \epsilon(|(A^+x)_i| + 1) \forall i \in [p]\} \quad (11)$$

Following the defaults in Keskar et al. [21], we take A as $\mathbb{I}_{n \times n}$. Using 32768 samples from MNLI validation_matched, we evaluate the initial loss $f(x)$. We use the same samples to compute the maximum loss $\max_{y \in \mathcal{C}_\epsilon} f(x + Ay)$, using an SGD optimizer with a learning rate of 8×10^{-5} , a batch size of 32, and accumulating gradient over 4 batches. In order to compute maximum loss, we perform a total of 8192 gradient updates, each followed by clamping of the weights within \mathcal{C}_ϵ . We set ϵ to 1×10^{-5} .

G Training loss

Even without any validation or test set to analyze, we can use the training set alone to make predictions about a model’s generalization strategies. Fig. 12 shows a strong relation between training loss convexity gaps and performance on HANS-LO. Future work can develop methods for predicting generalization early based entirely on training behavior.



(a) Clusters are based on convexity gaps in the MNLI training loss surface. Best squares fit shown.

(b) Color indicates convexity gap. Models on axes are sorted according to OOD performance.

Figure 12: Relationship between $\mathcal{C}\mathcal{G}$ on the MNLI training loss surface and accuracy on the HANS-LO diagnostic set.

H In-Domain Generalization

train	test	f	μ_{C_1}	σ_{C_1}	μ_{C_2}	σ_{C_2}	$\frac{\mu_{C_1} - \mu_{C_2}}{\sigma_{C_1}}$	$\frac{\mu_{C_1} - \max_{w \in C_2} f(w)}{\sigma_{C_1}}$
MNLI	MNLI	acc	0.844	0.002	0.839	0.002	2.50	1.00
MNLI	HANS-LO	acc	0.301	0.110	0.096	0.033	1.86	1.30
QQP	QQP	F1	0.879	0.001	0.872	0.002	7.00	5.00
QQP	PAWS-QQP	F1	0.436	0.005	0.424	0.004	2.40	0.60
CoLA	CoLA ID	MCC	0.601	0.017	0.600	N/A	0.06	0.06
CoLA	CoLA OOD	MCC	0.537	0.015	0.576	N/A	-2.60	-2.60

Table 1: Cluster mean, standard deviation, and distribution overlap for all tasks on both ID and OOD performance under metric f . C_1 is the larger cluster on each task. On CoLA, C_2 contains only a single model.

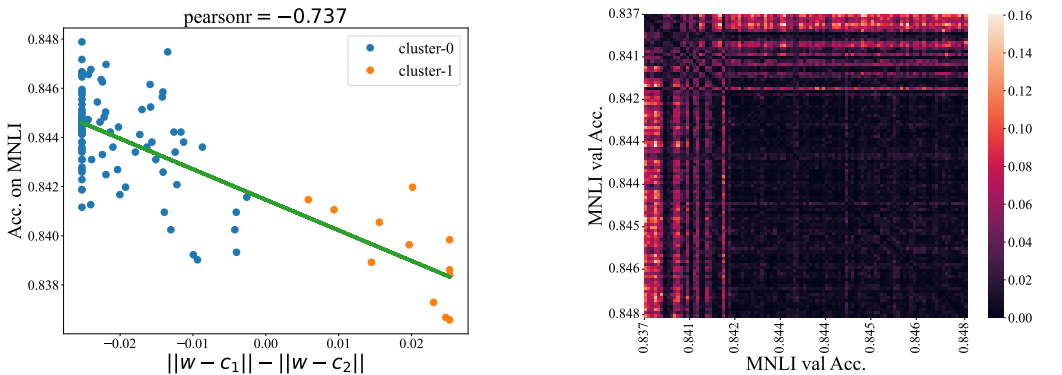
Let us consider the skeptical position that basin membership does not directly relate to OOD generalization strategies, but instead OOD performance is mediating the effect of general model quality in-domain. While ID (on MNLI) and OOD (on HANS) performance are certainly positively

correlated (Appendix E), we find that all 12 of the models in the syntax-unaware cluster fall at least 1.3 standard deviations below the mean of the syntax-aware cluster’s performance on HANS-LO (Table 1), and only 1 standard deviation below the mean on MNLI validation. The partitions are also less clear in the ID metrics (Fig. 13) compared to lexical overlap. Therefore, considered as a binary class, basin membership is more predictive of OOD behavior than of ID on NLI. Furthermore, the fact that performance on HANS-constituent is *negatively* correlated with ID performance (Appendix E) makes it clear that the underlying difference between these clusters is syntax-awareness, not overall model quality.

CoLA presents even stronger evidence for interpreting basin membership as related to OOD generalization over ID. The single outlier model falling outside of the main basin is a full 2.6 standard deviations outside the mean on OOD performance, but only 0.6 on ID performance.

However, we should not dismiss the relationship between ID accuracy and cluster membership. Compared to the diagnostic set PAWS, the ID validation set is more predictive of $\mathcal{C}\mathcal{G}$ on QQP (Fig. 14). In both MNLI and QQP, the relationship between ID and centroid distance also seems more linear than OOD.

An important caveat is the fact that ID evaluation and ID convexity gap measurements are performed on the same validation set, because the test sets are not public for these datasets. Therefore, ID performance is exposed during the clustering process, casting some doubt on alignment between the clusters and ID performance.



(a) Clusters are based on convexity gaps in the MNLI validation loss surface. Best squares fit shown.

(b) Color indicates convexity gap. Models on axes are sorted according to ID performance.

Figure 13: Relationship between $\mathcal{C}\mathcal{G}$ on the MNLI in-domain validation loss surface and in-domain validation accuracy.

I Alternative barrier measurements

In Fig. 15 we show NLI model clustering using the original barrier height metric (Equation 3) from Entezari et al. [7]. We can see that the Pearson’s correlation coefficient is -0.49 , which is far lower in magnitude than correlation in the $\mathcal{C}\mathcal{G}$ -metric space.

We also show the results for another metric, viz. area under the interpolation curve (AUC), in Fig. 16. Although this shows the same Pearson’s correlation coefficient, the clusters are much less crisp in the heatmap. In order to compute AUC, we first subtract the lowest point on the curve from all points, and then compute the area under the shifted curve.

Finally, we consider the effect of Euclidean distance (Fig. 17). The clustering effect is extremely strong and predictive of generalization behavior. It is worth considering the possibility that basins trap the models in a way that forces them to have larger Euclidean distances, but those Euclidean distances are the property that most determines the generalization strategy of the model.

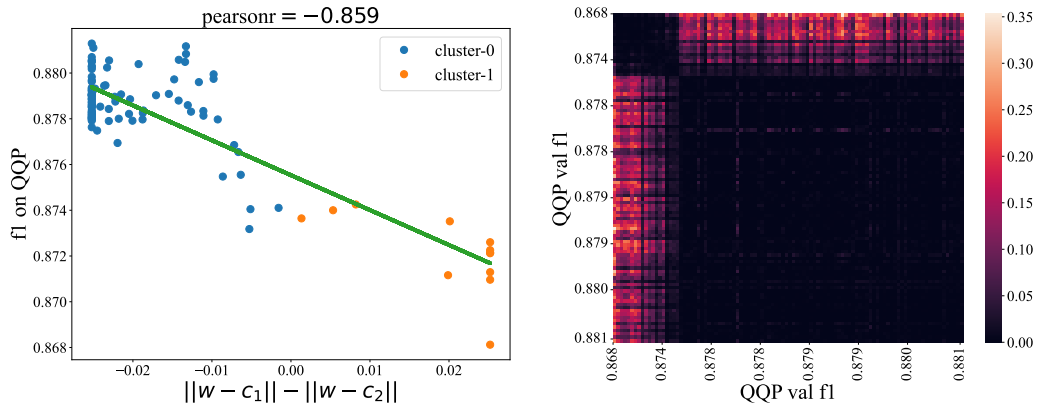


Figure 14: Relationship between \mathcal{C}_S on the QQP in-domain validation loss surface and in-domain validation accuracy.

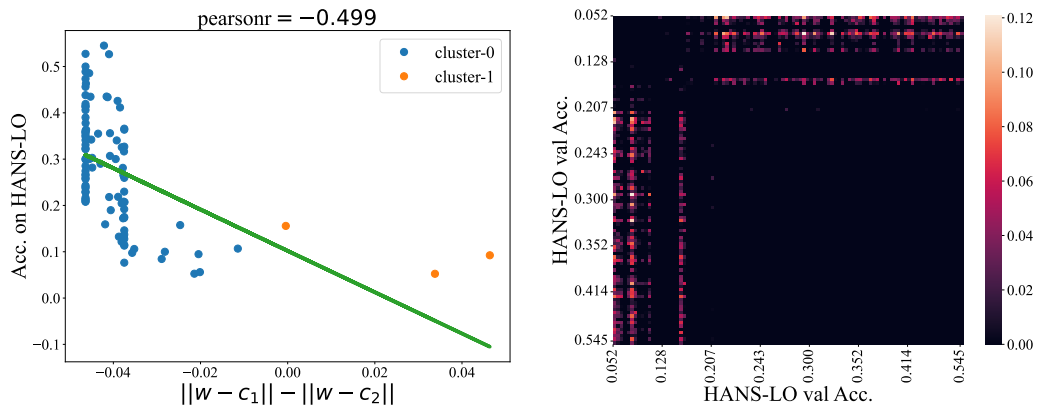


Figure 15: Relationship between \mathcal{B}_S on the MNLI validation loss surface and HANS-LO accuracy.

J Code and Models

We provide an anonymized version of our code at: <https://github.com/aNOnWhyMooS/connectivity> and all our fine-tuned models and evaluation as well as interpolation logs are released at: <https://huggingface.co/connectivity>.

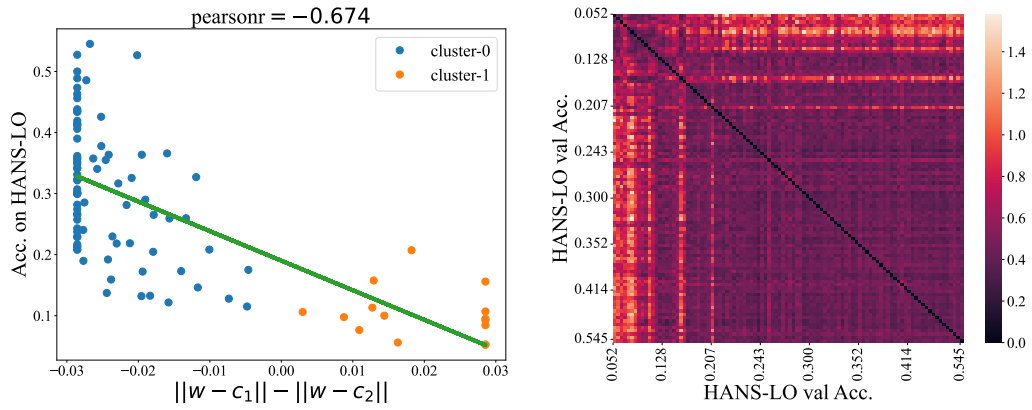


Figure 16: Relationship between AUC on the MNLI validation loss surface and HANS-LO accuracy.

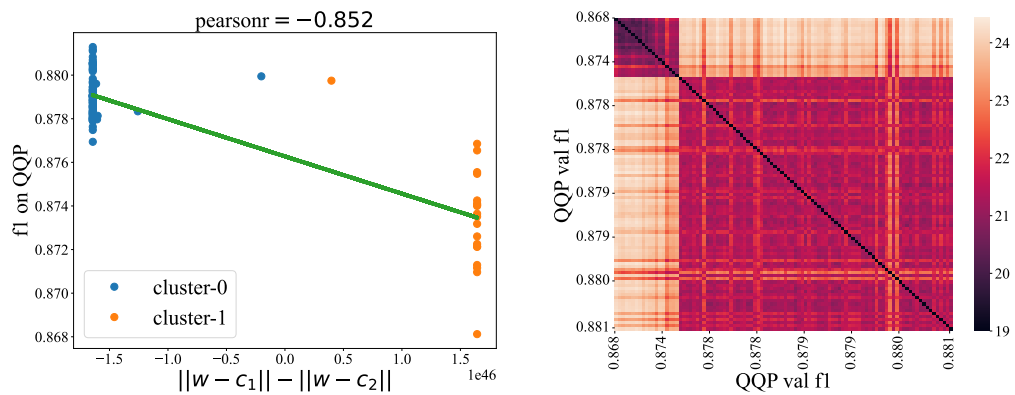


Figure 17: Relationship between Euclidean distance on the QQP validation loss surface and PAWS-QQP accuracy.